RESEARCH ARTICLE

Flowmeter accuracy: CFD analyses, experimental and field tests for two case studies of EPAL

André Morais[a], Miguel Fernandes[b] and Helena M. Ramos[c]

[a] *Master student of Civil Engineering at Instituto Superior Técnico, Technical University of Lisbon, Lisbon, Portugal*; [b] *Flow Measurement and Electrical Maintenance Manager, Maintenance Department, EPAL, Lisbon, Portugal*; [c] *Civil Engineering Department and CEHIDRO, Instituto Superior Técnico, Technical University of Lisbon, Lisbon, Portugal.*

Abstract: A team of engineers of EPAL identified some incongruenceses regarding flow measurement in two major hydraulic circuits: Castelo do Bode and Vila Franca de Xira. From the study developed a conclusion was reached which stated that the error of the measurement would be associated to the flowmeters in the pumping stations and the low accuracy would be connected to the perturbations induced by the geometry. In order to verify the source of the problem, and assess the hypotheses drawn, a CFD (Computational Fluid Dynamics) model, COMSOL Multiphysics, was used. The two hydraulic circuits were simulated using as boundary conditions the values measured *in situ*. To validate the results provided by the model, an intense campaign of experiments was developed. In this campaign two types of results were obtained: using an ultrasonic doppler velocimeter (UDV), the velocity distribution profiles were measured, which allowed the comparison of these profiles with the ones provided by the CFD; using the volumetric method and taking advantage of the flowmeters capability, an error evaluation was estimated. Lastly, having the model validated and calibrated, a new layout/geometry was proposed in order to mitigate the perturbations induced by the current geometry.

Key-words: flow measurement, flowmeters, CFD, turbulence, pipe geometry, flow perturbations.

1. Introduction

EPAL is the company that provides, maintains and manages the pipe network and the water, upstream from the inlet reservoirs and all the system until the consumers in the city of Lisbon, as well as several municipalities around it. Throughout the years, EPAL has installed flowmeters in several hydraulics circuits. As a result, management teams responsible for the system exploitation are able to control the in and outflow in those systems. The correct measurement of flowmeters is an extremely important factor in terms of company management. Amongst other domains of interest, the measured flow values are one of the key issues to detect leaks in the several systems. Therefore, for the company, the accuracy in flow measurement has significant impacts regarding both the planning and the investment decisions.

During the years, some incongruencies were notice regarding the records of flowmeters. This incongruencies would indicate the occurrence of leaks in pipes. Nevertheless, it was verified that pipes were tight. This conclusion implies that a new problem was not yet identified. Thus, in May of 2009, EPAL Direção de Gestão de Ativos - Departamento de Manutenção lead a study with the intention to obtain answers to this problem. The team studied two hydraulic circuits: between Vila Franca de Xira pumping station and A-dos-Bispos tank, and between Castelo do Bode pumping station and Asseiceira water treatment plant. The study undertaken did not reach any specific conclusions except that the problem would, most likely, be associated to the flowmeters measurement in the pumping stations.

This work has the objective to fulfil the need for answers to this problem: taking into account the study made, the collected information and the obtained results, an analysis to the variables which can disturb the flow is carried out, namely the pipes geometry and the way it can disturbs the flow and the register of the flowmeters. To fulfil such goal, a CFD model was used to simulate the flow in the hydraulic circuits. The conclusions reached are presented in this paper.

2. Turbulence and turbulent flow

Below a critical Reynolds number, 2000, the flow behaves in a orderly manner, laminar flow. For a Reynolds number higher than 2000, the flow characteristics change: the flow motion becomes more and more unsteady and the flow tends to a random and chaotic behaviour, turbulent flow (Hinze, 1959).

According to Novais-Barbosa (1985), for turbulent flows the flow variables change in intensity and direction, throughout the time, in a large flow region. Hence, the characteristic variables of the flow (i.e. velocity and pressure) are written as the sum between the mean value variable, with the corresponding fluctuating part (Versteeg and Malalasekra,

2007). Figure 2.1 represents an example of the described property for a velocity measurement in a turbulent flow.

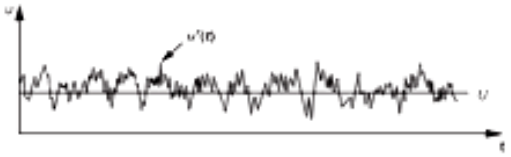

Figure 2.1 - Typical velocity measurement for a turbulent flow - U represents the average velocity while u'(t) represents the fluctuating velocity component (adapted from Versteeg and Malalasekra, 2007).

Other characteristic of the turbulent flow concerns its well marked tri-dimensional behaviour which is due to the turbulent fluctuating components (Lumley, 1992). In addition, vortexes, or turbulent eddies, with a wide range of length scales are moving inside the flow (Figure 2.2) which originate tri-dimensional fluctuations in all the properties of the flow (Tenneks and Lumley, 1972).

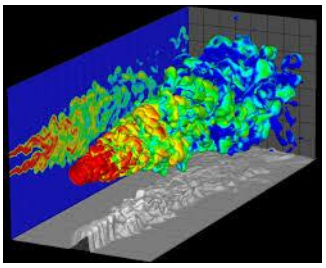

Figure 2.2 - Schematic image of the turbulent flow vortexes.

The eddies motion and the fluctuating components bring together or send away particles that were far from or close to each other, respectively. Therefore, mass, heat and momentum are exchanged in a very rapid and effective way (Çengel and Cimbala, 2006).

Large turbulent eddies interact with the flow mean energy by a process called vortex stretching (Tritton, 1988). Once velocities gradients exist within the flow, the eddies are distorted and stretched, because one end is moving faster than the other. Large scale turbulent eddies are influenced by the inertial forces and the viscous effects can be neglected (Bradshaw, 1973). The large eddies will create smaller ones providing, in this process, energy to maintain the turbulence (Batchelor,1967). For the smaller scale eddies the viscous and the inertial effect are equally relevant. For them, the system produces work against the viscous stress. Thus, energy is dissipated, leading to the increase of energy losses (Pope, 2000). This is the same to say that, once turbulence begins, the turbulent flow is able to maintain itself since it can produce new eddies to replace those disappeared. Hence, turbulence is self-sustaining (White, 1991).

3. Electromagnetic flowmeters

Flowmeters are one of the most important and used tools to measure, accurately, the volume flow rate (ISOMAG). Nowadays there are several kinds of flowmeters, but the most important for flow measurement are the electromagnetic and the ultrasonic ones. They are characterized for their high accuracy and self monitoring. The flowmeters used in EPAL, and studied in this work, are electromagnetic ones; thus, the following paragraphs will address its main characteristics and operating principle.

According to Frenzel *et al.* (2011), electromagnetic flowmeters are only disturbed by existing particles that may change the magnetic properties of the fluid. Properties like temperature, viscosity and the fluid density do not affect the measurements. However, as mentioned in Quintela (2002), the existence of parallel flow paths or streamlines (steady regime) is the necessary condition to guarantee accurate measurements.

These flowmeters have two different parts/elements: the primary and the convertor (Figure 3.1).

a) b)

Figure 3.1 - Examples of the electromagnetic flowmeters components - a) primary element; b) convertor (adapted from Frenzel *et al.*, 2011).

The first element corresponds to a hollow circular pipe with coils along its length and is set in the pipeline. The flow passing through the section creates an electromagnetic field which is proportional to the volume flow rate itself. The convertor is the brain element: it creates a magnetic field, reads the voltage, displays data and generates outputs. The convertor displays the volume flow rate and the volume passed through. These data are transmitted to the EPAL data center, which makes possible the remote management of the system, with a greater efficiency.

In order to measure the volume flow rate, electromagnetic flowmeters make use of Faraday principle. In

1831, Michael Faraday discovered that if an electric conductor is moving in a magnetic field perpendicular to the direction of the motion, an electrical current is induced, and that current is proportional to the magnetic field force as well as the motion velocity. If the conductor is water, the flow passing through a magnetic field induces an electrical current proportional to the flow velocity. Figure 3.2 represents the operating principle.

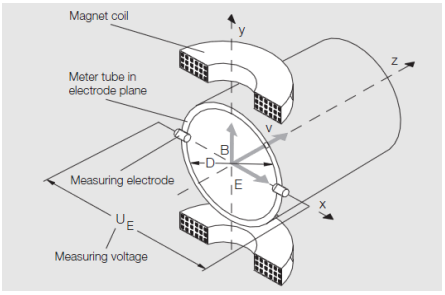

Figure 3.2 - Operating principle of an electromagnetic flow meter (adapted from Frenzel *et al.*, 2011).

Through mathematical manipulation, it yields that the electrical current, U_E, induced by the flow passing is directly proportional to the value of the volume flow rate, Q, or:

$$U_E \sim Q$$

According to Frenzel *et al.* (2011), the electrical current induced by the flow is taken into account only in the cross section defined by the electrodes, perpendicular to the flow. In other words, only the parallel component of the velocity is relevant for the volume flow rate measurement. This means that the flow tri-dimensional nature is disregarded.

The flow velocity profile is not the same throughout the entire cross section. For that reason, to prevent over or under-evaluations of the flow velocity the suppliers of these equipments use a weighting factor, W. Figure 3.3 represents the weighting factor distribution in the cross section..

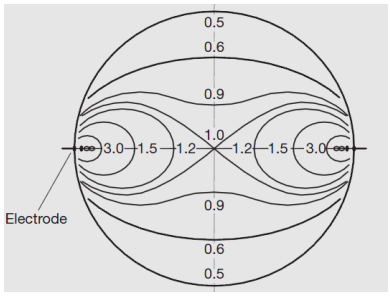

Figure 3.3 - Weighting factor distribution W in the electrode plane (adapted from Frenzel *et al.*, 2011).

Through analyses of Figure 3.3, each point in the cross section has a different weighting factor associated. The sum of the product between the velocity and the respective weighting factor corresponds to the electrical current, which is proportional to the volume flow rate. Despite being a good method to determine the volume flow rate in an homogenous magnetic field constant throughout with symmetric velocity profiles, this formulation does not provide good results for non symmetric velocity profiles. In these cases it would overevaluate some values and underevaluate others. This would lead to a non real volume flow rate.

To avoid this problem, the suppliers of the equipment considerate a magnetic induction field, B, inversely proportional to the weighting factor W, equation [3.1].

$$W \cdot B = const \qquad [3.1]$$

According to equation [3.1], for a cross section region in which the weighting factor is small, the magnetic induction field is increased, and vice versa. This action ensures good results even for none symmetrical velocity profiles.

4. CFD and experimental analyses

4.1. CFD model

CFD is the computer based simulation analyses of systems involving fluid flow. These simulation tools represent an important technological advance towards the detailed flow understanding, allowing theoretical considerations regarding the physical behaviour of the flow, with mathematical formulations for tri-dimensional modelling and analyses (Abbot and Basco, 1989). These models make possible, not only to approximate the behaviour of turbulent and laminar flows, but also the multiple ways of energy transference, the flow phase changes, the vorticity, the turbulence levels, among others possibilities (Fletcher, 1991).

The CFD used in this work was COMSOL Multiphysics (hereinafter referred as COMSOL) which presents accurate results for several fluid flow problems (Georgescu *et al*., 2007). COMSOL is a finite element method program, who uses the mass conservation and the RANS (Reynolds averaged Navier-Stokes) equations as governing flow equations. The finite elements method is a computational method that divides an object into smaller elements. Each element has assigned a set of characteristic equations that are then solved as a set of simultaneous equations to estimate the behaviour of the object (COMSOL 4.3, 2012). From the available models, the one used was the k-ε model. The k-ε models (Speziale, 1987) are the most common and most used models worldwide because of the good results they present.

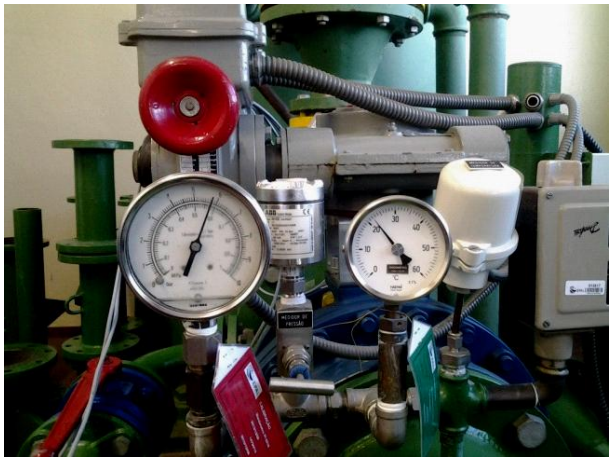

a)

b)

Figure 4.1 - Laboratory layout - a) inlet - manometer (left) and thermometer (right); b) three reference flowmeters (blue arrows).

The boundary conditions represent the problem physical borders. For the model used, three types of boundary conditions were considered: inlet, outlet and solid walls. The in and outlet conditions were chosen from the several possible in such a way that optimized the data available. For that reason the inlet boundary condition was the pressure, while the outlet boundary condition was the average velocity. The boundary condition related to the walls was the no-slip condition, which stated that the walls were impermeable.

One of the most important steps in CFD modulation corresponds to the mesh definition. It has as purpose the discretisation of the geometry into smaller units, called mesh elements. Its resolution and element quality are important aspects to take into account when validating a model, since the decreased of resolution can originate low accurate results (Gresho, 1991), meanwhile, low mesh element quality can led to convergence issues (Lumley, 1978).

COMSOL has built in the option of physics-controlled mesh. The physics-controlled mesh defines, automatically, the size attributes and operations sequences necessary to create a mesh adapted to the problem physics. These physics-controlled sequences are based on heuristics as well as the knowledge of experts gathered in several investigations.

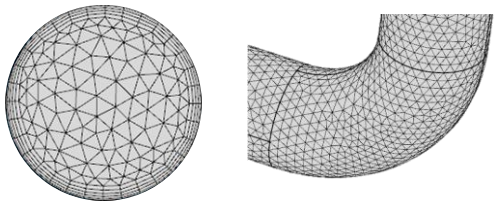

a) b)

Figure 4.2 - Mesh examples: a) Boundary layer mesh; b) Refinement near a curve.

For the fluid-flow model, since the mesh is adapted to the physic setting, the mesh is finer than the default one, with a boundary layer (Figure 4.2 a)) along its boundaries in order to solve the thin layer near the solid walls where the gradients of the flow variables are high (Bakewell *et al.*, 1967; Wosnik, Castillo and George, 2000).

4.2. Experiments

In order to assess the computational results provided by the CFD model, an intense campaign of experiments were developed to validate them. The case studies corresponded to two major EPAL hydraulic circuits and for that reason the experiments were limited. Therefore, to complement the analyses, some experiments were developed in EPAL laboratory in order to compare and validate the computed simulations with the experimental results. This experiments did not take into account the installation recommendations of Associação Portuguesa de Distribuição e Drenagem de Águas (2000) and the EN 14154.

Several experiments were developed with the intent of mimicking a large number of geometries that could induce perturbations. To assess if the results provided by the model were accurate, several ultrasonic doppler velocimeter (UDV) measurements were made which provided velocity distribution profiles. The position of the UDV was changed in order to have more than one section where the results comparison could be made. The same happened with the flowmeters: their position was changed to assess how different straight distances would influence the reading.

The experiments took place in EPAL laboratory, Laboratório de Contadores de Água, at Olivais, Lisbon. The

CFD boundary conditions were imposed by the facility constrains and equipments. The inlet was the pressure measured upstream by a manometer, meanwhile the outlet condition was the volume flow rate verified downstream by flowmeters of reference (Figure 4.1).

Downstream the flowmeters, there are two high accuracy tanks (Figure 4.3). These tanks are certificated and calibrated in a traceable laboratory using the International System of Units. After the experiment concluded, the volume of water read in those tanks was used to calculate the error of the flowmeters, through the volumetric method.

a) b)

Figure 4.3 - High accuracy tank - a) 1000 m^3 b) 5000 and 10000 m^3 (yellow arrow).

The procedure followed in the several experiments consisted in the following steps: the water was pumped from the drinkable water tanks to the laboratory, at a pressure of, approximately, 6 bar. The experiments started after some minutes have passed to guarantee that the flow was under steady state conditions. The velocity profile was measured with the UVD and the initial volume and the final one were registered as well as the pressure and the duration of the experiment. When all the information was measured and the data registered, the first experiment was concluded. For the same geometry, the position of the flowmeter was changed and the procedure repeated. When the measurement was concluded in all the required points, and when the flowmeter results in the several sections tested were registered, the geometry was changed and the procedure repeated until all geometries and tests were developed.

The profiles measurement with the UDV were most of the times quite toilsome. The reason for it was the good water quality of EPAL. In tests like the ones made, it is advisable to introduce some particles (this phenomenon is called seeding) in order to have a better reflexion of the ultrasonic wave. Since the water used in the tests was treated water, directly from the tanks that make the distribution, seeding was out of question. Since the water was very clean the UDV measurements were very difficult. Several trials needed to be made in order to the UDV be able to provide reasonable profiles.

The testes developed and presented in this paper are presented in Table 4.1.

Table 4.1 - Schematic test notation.

Notation		Scheme	Observations	
Geometry 1	**Type 1**	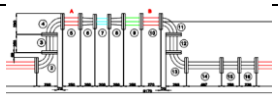	Vertical plan perturbation. DN80 flowmeter - colour blue; DN100 flowmeter - colour green.	UDV measurements in the red pipes identified by A and B.
	Type 2	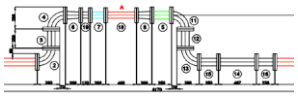		UDV measurements in the red pipes identified by A. Perturbation due to vertical curves with a small distance to dissipate before the DN80 flowmeter.
	Type 3	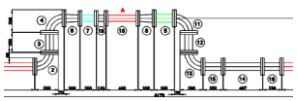		UDV measurements in the red pipes identified by A. Perturbation due to vertical curves without any straight distance from the DN80 flowmeter.
	Type 4	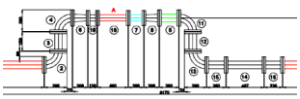		UDV measurements in the red pipes identified by A. Perturbation due to vertical curves with a long straight distance from the DN80 flowmeter.
Geometry 4	**Type 1**	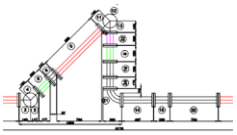	Three plans perturbations. DN100 flowmeter - colour green.	Perturbation due to vertical curves and rotation of the vertical orthogonal axis.

4.3. Comparisons

Some results from the large series of tests developed are presented in the Figures 4.4 to 4.12.

Regarding the simulation presented in Figure 4.7 the profiles for the volume flow rate of 12 m^3/h were not carried out. Despite being the second experiment presented, following the design order, these experiments were the last to be made. The profiles measured for the 100 m^3/h are presented in Figure 4.8.

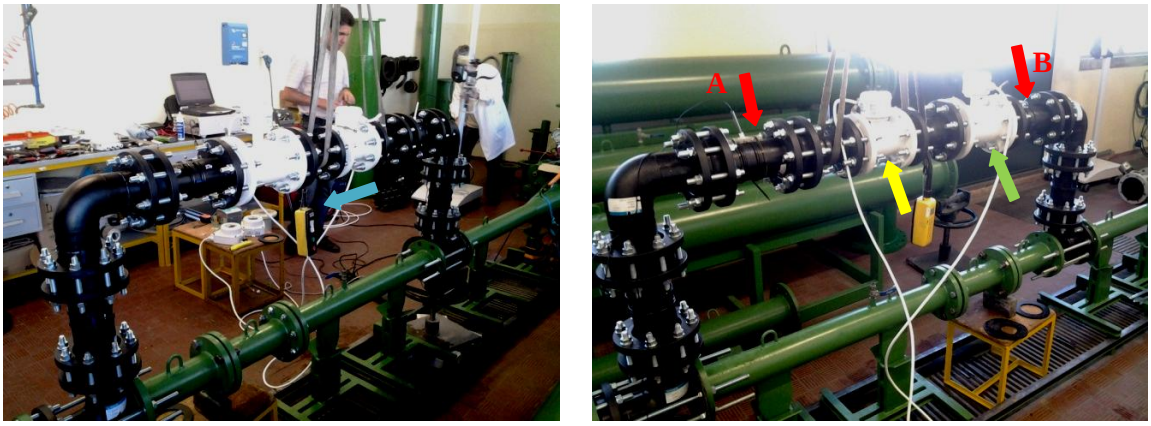

a) b)

Figure 4.4 - Geometry 1, type 1 experiment - a) experiment layout (flow direction identified by the blue arrow); b) experiment layout detail - DN80 flowmeter identified by the yellow arrow, DN100 identified by the green arrow. The UDV probe measured in the pipe sections identified by the red arrows (probe installed in the pipe identified by the red A arrow).

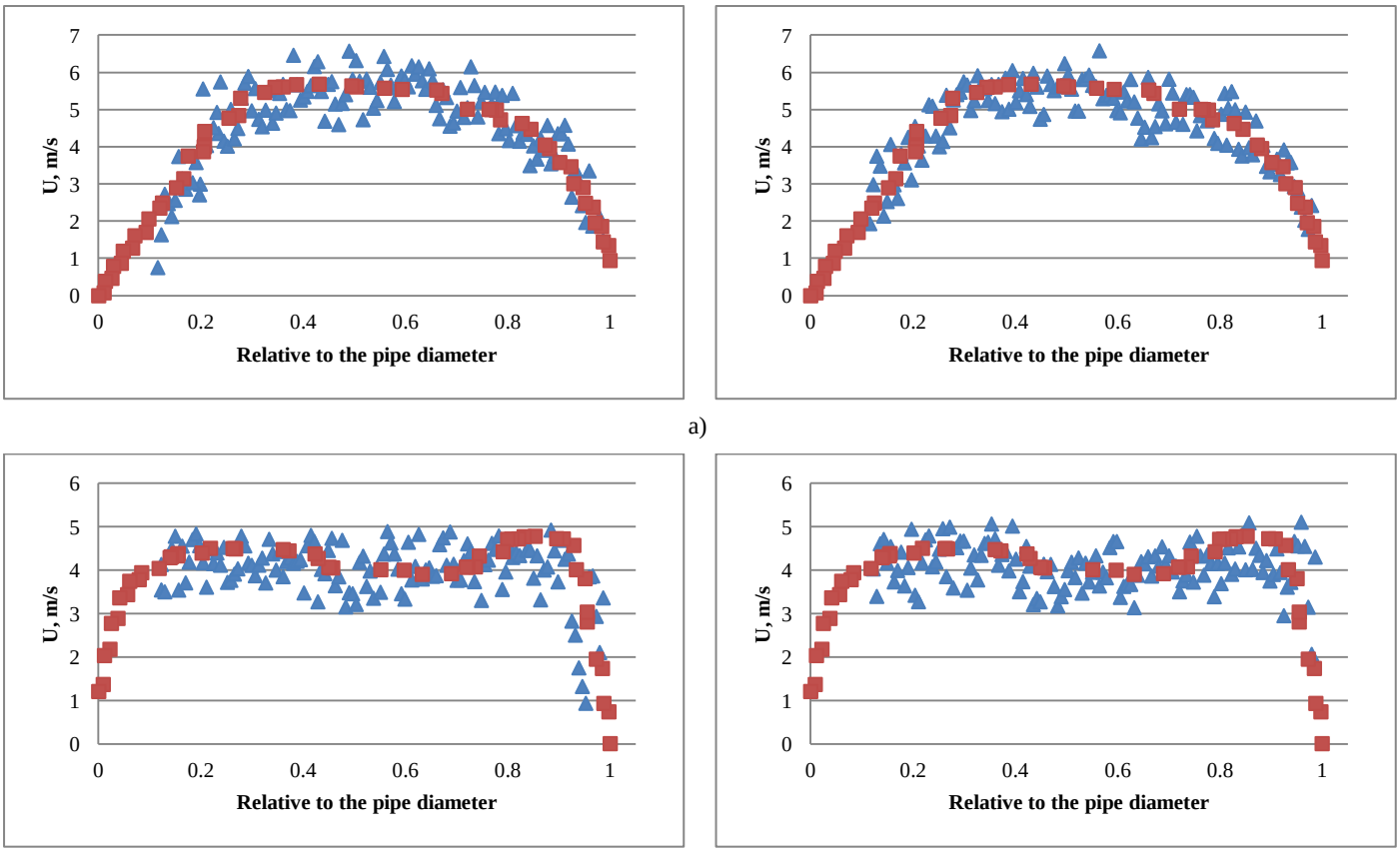

a)

b)

Figure 4.5 - UDV profiles for 100 m^3/h for Geometry 1, type 1 (blue triangles - experimental results; red squares - simulated results) - a) profiles measured in the location identified as A in Figure 4.4; b) profiles measured in the location identified as B in Figure 4.4.

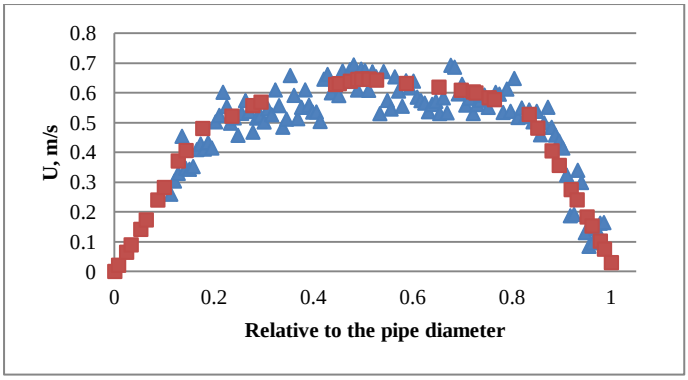

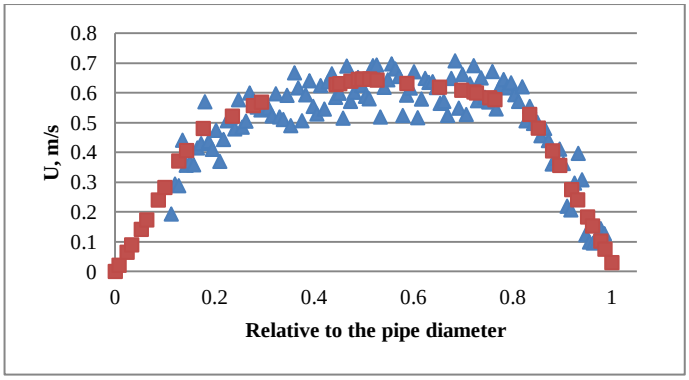

a)

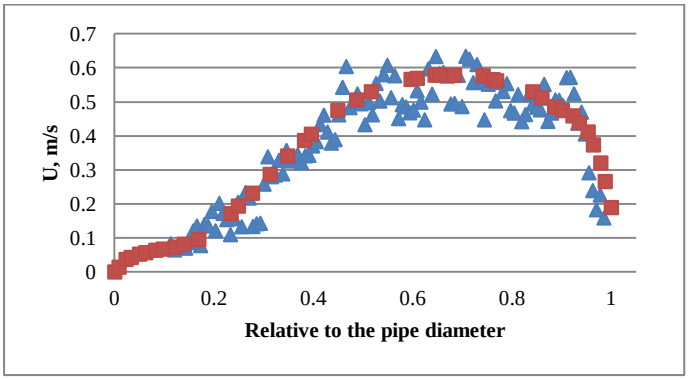

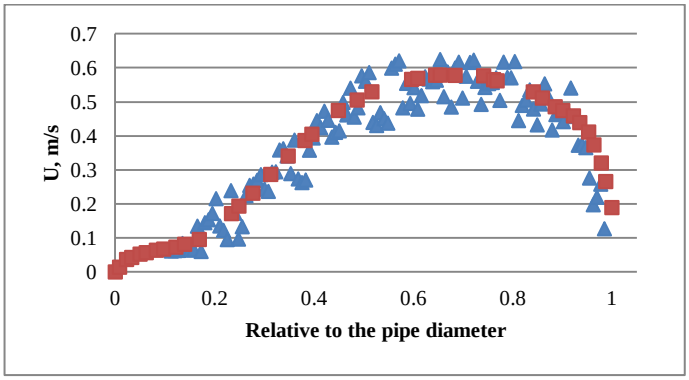

b)

Figure 4.6 - UDV profiles for 12 m^3/h for Geometry 1, type 1 (blue triangles - experimental results; red squares - simulated results) - a) profiles measured in the location identified as A in Figure 4.4; b) profiles measured in the location identified as B in Figure 4.4.

a)

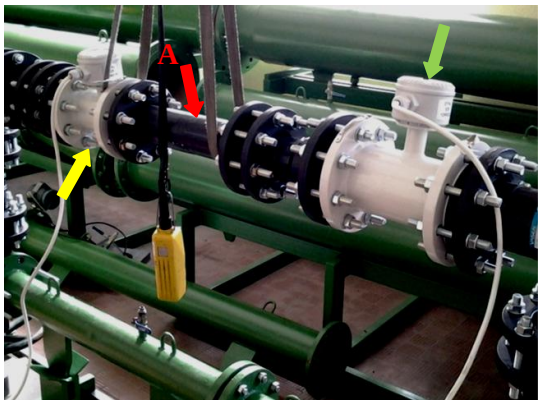

b)

Figure 4.7 - Geometry 1, type 2 experiment - a) experiment layout (flow direction identified by the blue arrow); b) experiment layout detail - DN80 flowmeter identified by the yellow arrow, DN100 identified by the green arrow. The UDV probe measured in the pipe section identified by the red arrow.

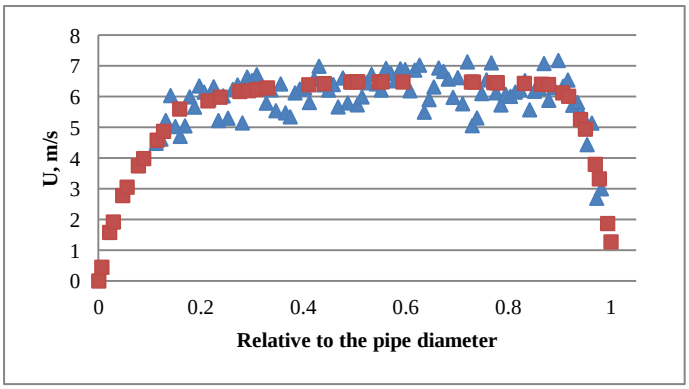

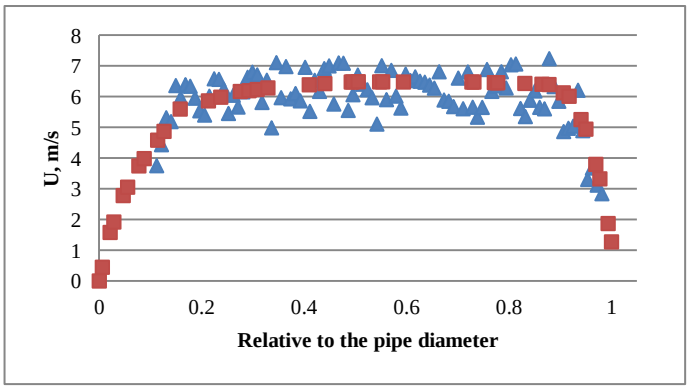

Figure 4.8 - UDV profiles for Geometry 1, type 2 measured at the location identified as A in Figure 4.7 for 100 m^3/h (blue triangles - experimental results; red squares - simulated results).

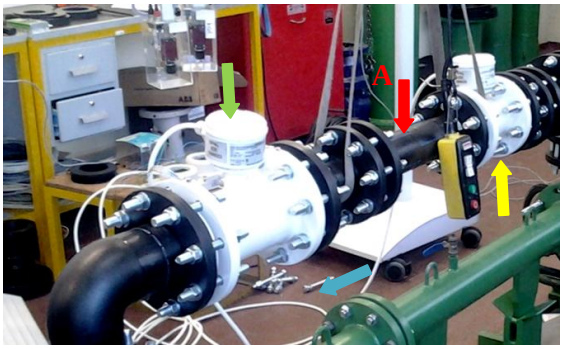

Figure 4.9 - Geometry 1, type 3 experiment - flow direction identified by the blue arrow; DN80 flowmeter identified by the yellow arrow, DN100 identified by the green arrow. The UDV probe measured in the pipe section identified by the red arrow.

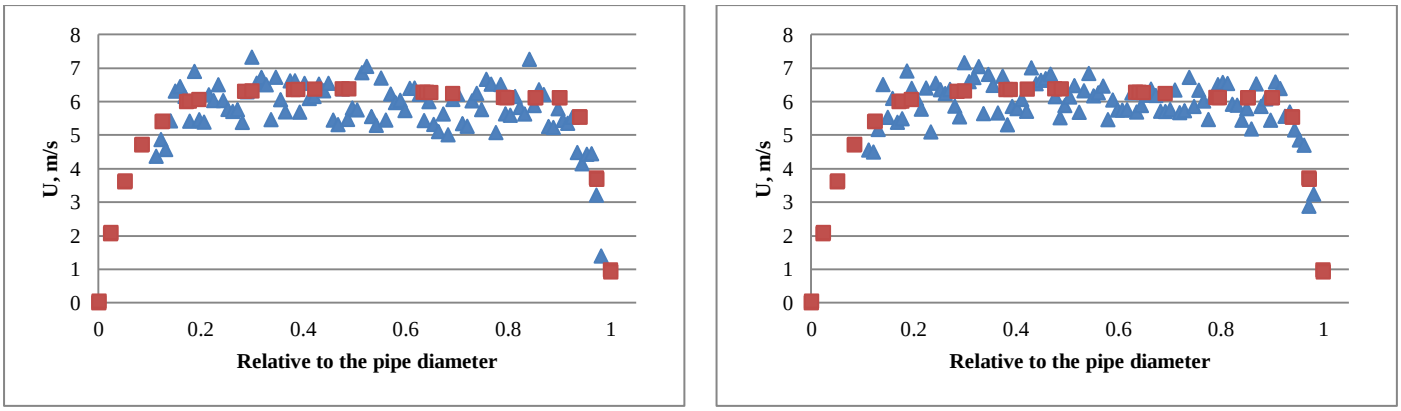

a)

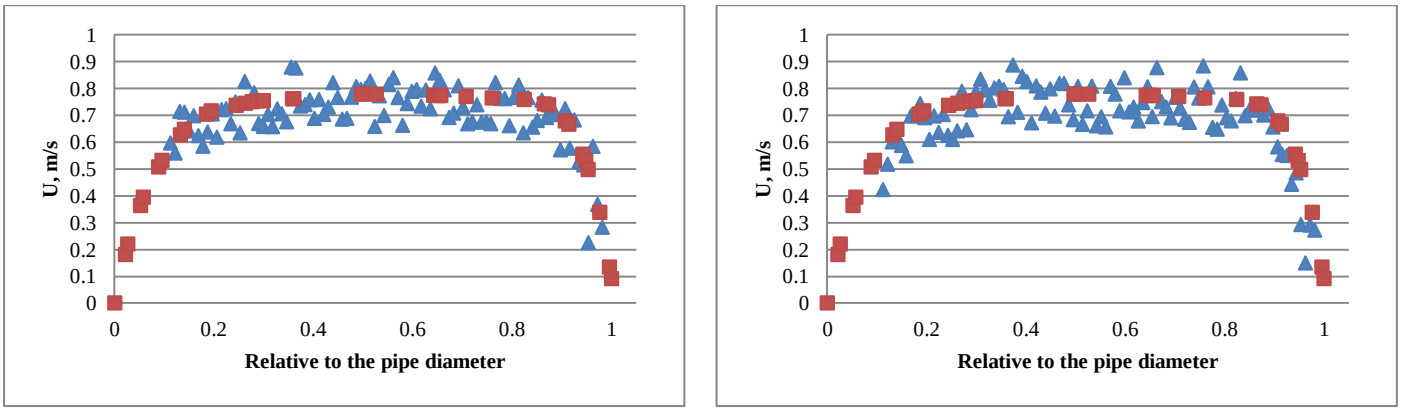

b)

Figure 4.10 - UDV profiles for Geometry 1, type 3 measured at the location identified as A in Figure 4.9 (blue triangles - experimental results; red squares - simulated results) - a) 100 m^3/h; b) 12 m^3/h.

For the Geometry 1, type 4 experiment, Figure 4.11, the 12 m^3/h profiles were not presented because the results were not adequate. The profiles obtained were very chaotic and nil in almost every point. The justification for this was, very likely, due to the existence of air between the ultrasonic probe and the pipe wall. The probe cannot be in contact with air, otherwise it could not measure. To avoid it, a gel was introduced in order to prevent this situation. Nevertheless, when the experiment was taking place the gel might have been insufficient and the problem was not detected. Only when the results analyses were made the problem arose. Since the UDV was no longer available at EPAL laboratory, there were no profiles to present for the 12 m^3/h for the Geometry 1, type 4 simulations. The 100 m^3/h computed results are similar to the experimental ones (Figure 4.12).

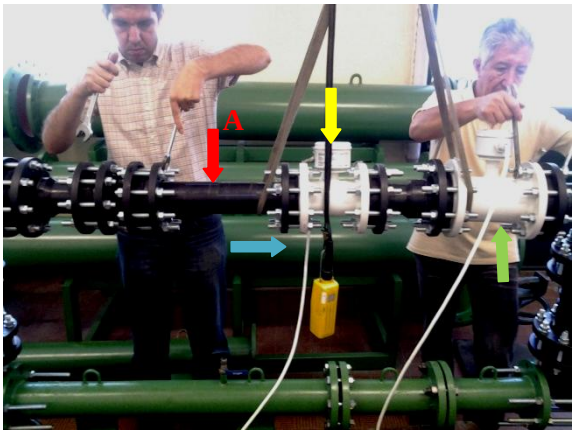

Figure 4.11 - Geometry 1, type 4 experiment - experiment layout detail - flow direction identified by the blue arrow. DN80 flowmeter identified by the yellow arrow, DN100 identified by the green one. The UDV probe measured in the pipe section identified by the red arrow.

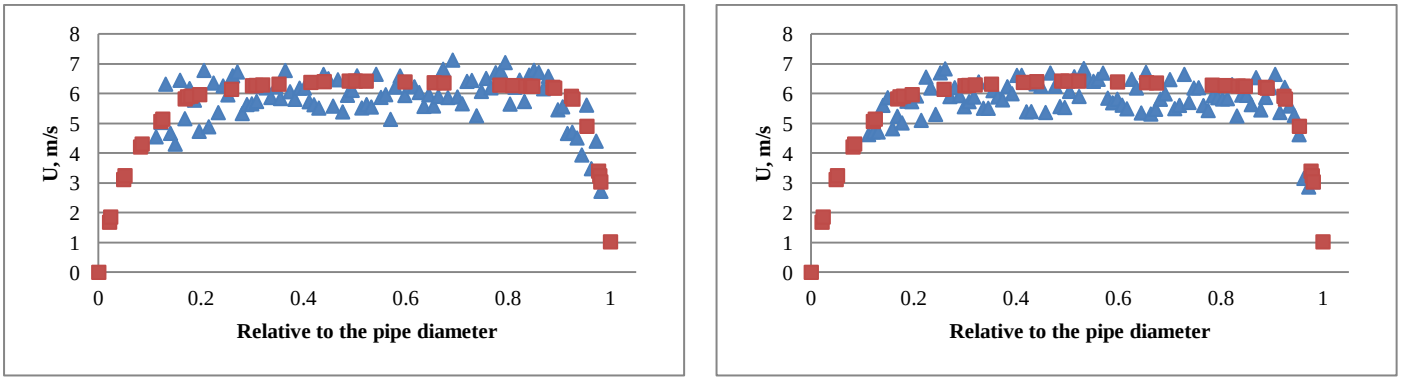

Figure 4.12 - UDV profiles for Geometry 1, type 4 measured at the location identified as A in Figure 4.11 for 100 m^3/h (blue triangles - experimental results; red squares - simulated results).

Through the comparison between the profiles obtained with the UDV and those computed by the model it is clear that the profiles are similar. These results allow to conclude that the CFD model is validated and makes possible the assumption that for other simulations, if mesh features, types of boundary conditions and materials properties remain the same, the model would provide good results. Thus, according to these remarks, the results achieved are validated.

Table 4.2 represents the errors of the flowmeters calculated by the volumetric method (experimental error) and the ones calculated with the spreadsheet developed (model error).

Table 4.2 - Values of the errors calculated with the volumetric method and the spreadsheet one, for Geometry 1 and respective flowmeters.

	Q = 100 m^3/h				Q = 12 m^3/h			
	Error				Error			
	Experimental		Model		Experimental		Model	
Test	DN100 [%]	DN80 [%]	DN100 [%]	DN80 [%]	DN100 [%]	DN80 [%]	DN100 [%]	DN80 [%]
Type 1	-0.40%	0.64%	-0.48%	0.71%	-1.18%	-0.20%	-1.27%	-0.55%
Type 2	1.88%	0.48%	1.11%	0.41%	2.65%	-1.57%	1.61%	-1.48%
Type 3	0.52%	-1.68%	1.11%	-1.76%	1.47%	-2.16%	1.61%	-2.08%
Type 4	0.94%	0.08%	1.11%	0.16%	0.69%	1.37%	1.61%	0.75%

For the volume flow rate of 100 m^3/h for the DN 100 flowmeter, it is verified that the error associated to type 1 is the smallest error. Changing the position of the flowmeter, maintaining the volume flow rate, the errors vary. The position of the flowmeter in experiments type 2, 3 and 4 remained constant. Only the upstream layout was slightly changed. If the geometry remained completely the same, and since the errors changed, the logic conclusion was that the DN100 flowmeter

had low repeatability. The repeatability phenomena is an important one for every industry which requires accurate measurements. Measurement repeatability is the property of an equipment which for the same test conditions, it presents very similar errors. Since the geometry changes slightly, the conclusion is not entirely valid.

The difference of errors verified in type 2, 3 and 4 for the experimental results may be due to some minor installation problems (such as the position of the gasket inserted in between the flanges which can obstruct a small part of the pipe) that, since the model was not developed with such detail level were not assessed by the computed results but were assessed by the flowmeter. For this reason the errors calculated with the computed results remain the same for the three tests. The commentaries of the results concerning the same flowmeter, for a 12 m^3/h volume flow rate, are analogous to the presented.

The type 3 experiment is the one where the value of the error is the highest for the DN80 with a volume flow rate of 100 m^3/h. Of all the experiments made the type 3 experiment corresponded to the worst layout since the flow has not enough strait pipe length in order to dissipate the perturbation caused by the vertical curves. The type 1 and type 2 present very similar errors. The fact that the experimental error verified in type 1 is higher than the one verified in type 2 is surprising because the existence of 8º reduction/expansion cones (as occurs for this situation) is considered as good procedure by the flowmeters manufactures. The probable reason for this discrepancy can be installation problems. The type 4 experimental result present the minimum error, as would be expected, since the perturbations due to the upstream perturbations can be dissipated throughout the straight pipes.

Lastly, the results for the DN80 with a volume flow rate of 12 m^3/h behave as expected. The only out of ordinary situation is the one associated to type 4. As mentioned in the previous paragraph the error ought to be low. Nevertheless, the error is the same magnitude than the error of type 2. The justification for this must be, again, some problems in the installation, which may induce perturbations not simulated by the CFD model.

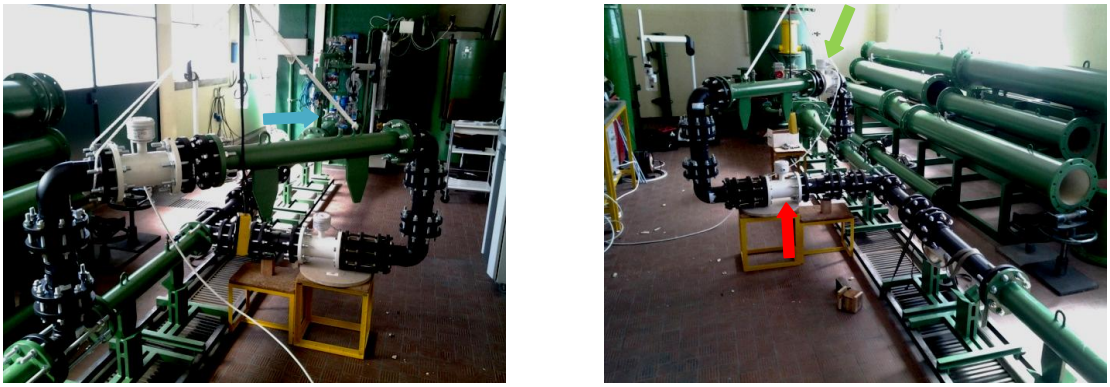

a) b)

Figure 4.13 - Geometry 2, type 1 experiment - a) upstream to downstream (flow direction identified by the blue arrow); b) downstream to upstream - DN100 flowmeter previously used identified by the green arrow, DN100 flowmeter used only in these tests identified by the red arrow.

According to the flowmeters manufactures the increase in velocity would originate an increase in accuracy. However, through analyses of Table 4.3 which assess the perturbations due to vertical curves and a rotation on the vertical orthogonal axis, it is clear that the error associated to the geometry is much higher than the increase on accuracy. While for 12 m^3/h the perturbations induce a small error, for the 100 m^3/h volume flow rate the error is very significant, around -28 %. This value is very odd since this flowmeter had never presented such an error. The justification for this value is most probably due to an extremely intense turbulence, which might have induced flow contraction which could have influenced, largely, the flowmeter measurement.

Through the results achieved it is reasonable to conclude that the pipes and flowmeters installation, are an important factor in flow measurement accuracy. The error associated to the position of the gasket, which may obstruct the pipes, are important and, in several situations, avoidable errors. In practice, since the number of gaskets is reduced, if the engineering good practice are followed it is possible to make sure that problems associated to installation error can be disregarded. However, in these experiments, since the number of gaskets was big, the error was not preventable.

The most relevant conclusion resulting of these experiments is that the error in flow measurement is due to the error associated to the flowmeter, to the error associated to the layout or geometry of the facility and to installation errors, associated to several hydraulic elements/components such as valves, disassembly joints, suction cups, among others, as well as the already mentioned gaskets.

Table 4.3 - Values of the errors calculated with the volumetric method and the spreadsheet one, for Geometry 2. Test 1. - new DN100 flowmeter (red arrow of Figure 4.13). Test 2 - DN100 flowmeter used in the previous tests (green arrow of Figure 4.13).

	Q = 100 m^3/h		Q = 12 m^3/h	
	Error		Error	
Test	Experimental	Model	Experimental	Model
Type 1, test 1	-2.08%	-2.15%	-1.08%	-1.01%
Type 1, test 2	-28.70%	-1.55%	-1.47%	-1.51%

5. Case studies

5.1. Castelo do Bode hydraulic system

The first case study was Castelo do Bode hydraulic circuit (CBC). Almost 90% of the total water volume comes from Castelo do Bode dam, which is then pumped in Castelo do Bode pumping stations 1 and 2. A schematic representation of Castelo do Bode facility is presented in Figure 5.1. The flow arrives by the drive pipe (right/left side of Figure 5.1 a)/b) respectively), and follows through the pump (represented by the green section) by a vertical pipe in the top of the drive pipe. Afterwards, the flow reaches the delivery pipe with a 30º angle, sidewise, having passed by two 90º curves.

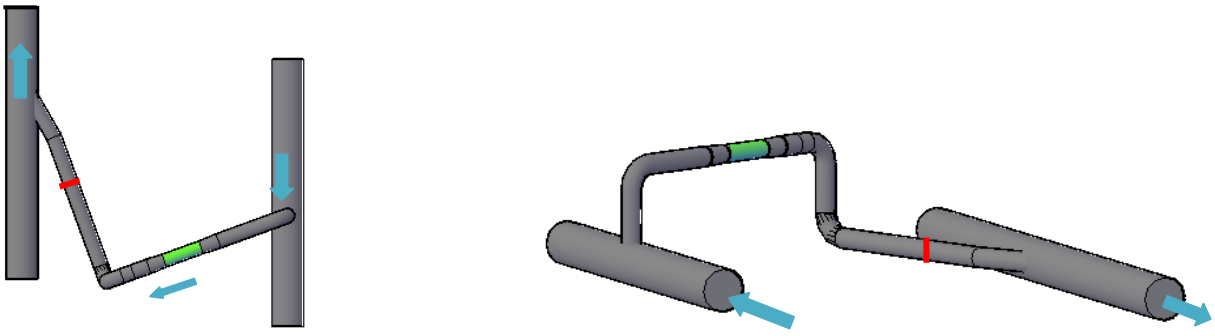

a) b)

Figure 5.1 - Schematic representation of the existing geometry in Castelo do Bode pumping station (pump location identified by the green pipe section; flowmeter identified by the red line; flow direction identified by the blue arrow) - a) Plan; b) 3D view.

The problems detected in 2009 were thought to be correlated to the flowmeters in the pumping station. Hence, the problem studied corresponded to the flow disturbances and the way they can influence the flow measurement. Since the flow passes though a pump, the disturbances from upstream were disregarded, i.e., the perturbations caused by the pump are the most significant for this analysis. Thus, the geometry used for simulating the disturbances corresponded to the one represented in Figure 5.2.

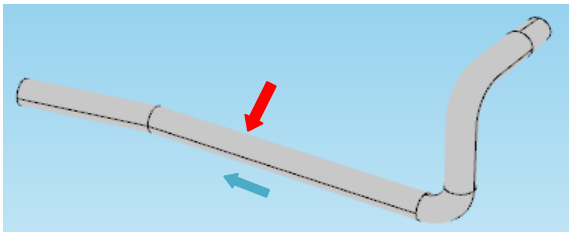

Figure 5.2 - Castelo do Bode modelling geometry - flowmeter section identified by the red arrow; flow direction identified by the blue arrow.

The characteristics of the pipes and of the flowmeters are presented in Table 5.1.

Table 5.1 - Characteristic of the main pipes and flowmeter for CBC.

Material	Steel
Expansion	DN700 to DN800
Remaining pipes	DN800
Flowmeter	DN800

The procedure followed to develop the simulations consisted in the definition of the geometry, after which was necessary to identify the characteristics of the fluid (i.e. water) and the boundaries conditions. Lastly the mesh definitions were chosen and if the problem was time dependent, or not. The geometry used is presented in Figure 5.2 and the boundary conditions and other important features are in Table 5.2.

Table 5.2 - CBC existing situation: simulation input values and characteristics.

Inlet	9.5 bar
Outlet	1.5 m/s
Wall	No-slip
Mesh	Physics-controlled
Flow conditions	Steady state

The streamlines velocity field are represented in Figure 5.3.

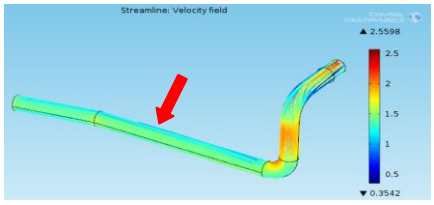

Figure 5.3 - Streamlines simulation along the hydraulic circuit for the CBC (flowmeter section identified by the red arrow), in m/s.

In Quintela (2002) to guarantee the measurement accuracy, the electromagnetic flowmeters require linear and rectilinear streamlines. In the flowmeter section, the streamlines appear to be parallel to each other. This factor would indicate that the flowmeter would present an accurate measure, however, that is not what was verified. The velocity distribution across the electrodes cross section of the flowmeter is represented in Figure 5.4. The velocity changes largely within the cross section: from zero near the wall to over 1.7 m/s in the right lower side, where the velocity attains the biggest value. This behaviour was not expected because the flow passes through two ninety degree curves after the pump, therefore, it would be reasonable to anticipate that the perturbations induced by them would be, in practice, nil, according to manufactures experience. Nevertheless, it is important not to forget the second curve has a rotation in the z axis. Therefore, the non-symmetric cross section seems to be due to the existing geometry.

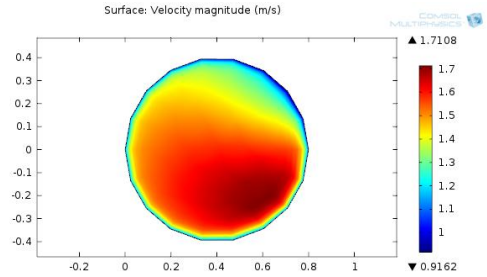

Figure 5.4 - Velocity distribution simulation in the electrodes cross section for CBC.

In order to estimate an error from a velocity distribution in the flowmeter cross section a procedure was developed that used the information from Figure 3.3. For each point provided by the model the correspondent weighting factor was estimated and multiplied. The velocity that would be measured by the flowmeter was estimated dividing the product of the velocity and the weighting factors by the sum of all the weighting factors.

$$Error = \frac{U_{calculated} - U_{boundary\ conditon}}{U_{boundary\ condition}} \quad [6.1]$$

The error associated to the flowmeter was calculated according to equation [6.1]. The value of the error for the existing layout was estimated equal to -0.71 %. The error calculated by EPAL, through water balances, is close to -1 %. Since the errors are alike the model is considered to be validated and the results accurate.

5.2. Vila Franca de Xira hydraulic system

Vila Franca de Xira hydraulic circuit (VFXC) is one of the most important facilities for EPAL, in a strategic point of view: all the water that arrives to Lisbon, and the surrounding municipalities is pumped in the Vila Franca de Xira pumping stations. Therefore a careful analysis of this circuit is quite important for the company efficiency.

The existing layout, represented by Figure 5.5, was adopted from EPAL existing blueprints.

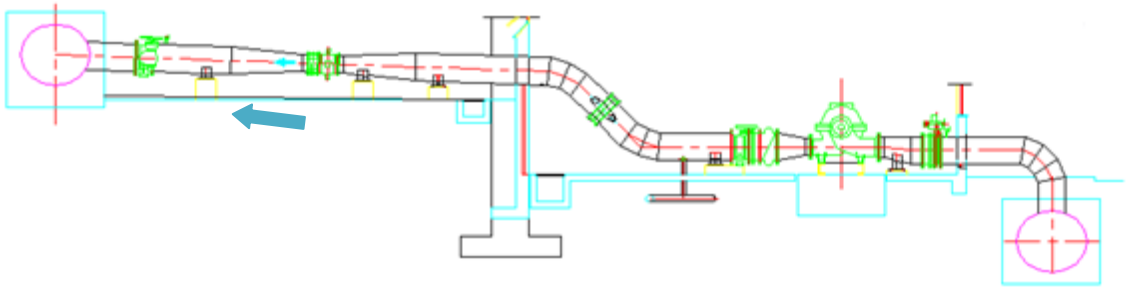

Figure 5.5 - Vila Franca de Xira side view from pumping station 2 (adapted from EPAL design draws) - flow direction identified by the blue arrow.

The flow is pumped from the driving pipe (right side of the figure), passes through an S shaped pipe (called horse neck), continues straight ahead, where there is a diameter reduction followed by the flowmeter. After the flowmeter, there is an expansion, and, afterwards, the pipe reaches the delivery pipe.

The geometry considered to assess the existing situation overlooked the pump and the upstream pipes. Figure 5.6 represents the modelling geometry used.

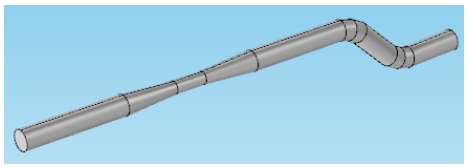

Figure 5.6 - Vila Franca de Xira modelling geometry.

The characteristics of the pipes and flowmeters are presented in Table 5.3 and the boundary conditions and other important features are presented in Table 5.4.

Table 5.3 - Physical characteristic of the main pipe and flowmeter for VFXC.

Material	Steel
Expansion/Reduction	DN800 to DN500
Remaining pipes	DN800
Flowmeter	DN500

Table 5.4 - VFXC situation simulation values and characteristics.

Inlet	14.1 bar
Outlet	1.96 m/s
Wall	No-slip
Mesh	Physics-controlled
Flow conditions	Steady state

In Figure 5.7 are represented the streamlines velocity field. Through a specific analyse of such figure, the horse neck induces a significant perturbation on the flow: the streamlines cross each other paths in a disorganized behaviour. When they achieve the reduction cone the streamlines tend to stabilize and became more and more parallel. In the flowmeter section the streamlines are parallel which is the theoretical necessary condition to guarantee a accurate measurement.

In Figure 5.8 is presented the distribution of the velocity across the flowmeter electrodes cross section. Comparing it to the CBC (Figure 5.4) it is apparent that for CBC the profile is much more distorted than for VFXC. While in CBC there are several curves and rotations in VFXC the major perturbation to the flow is the horse neck. Since for the VFXC the flow passes through a reduction cone, it tends to stabilize. For that reason the cross section is an almost constant one.

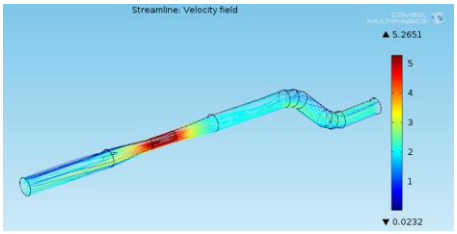

Figure 5.7 - Streamline simulation along the hydraulic circuit for the VFXC, in m/s.

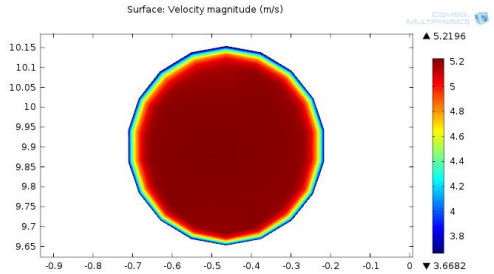

Figure 5.8 - Velocity distribution simulation in the electrodes cross section for VFXC.

The error estimated according to the procedure referred was 2.53 %. The error verified by EPAL team of experts was between 2 and 3 %, which means the results of the model are valid.

6. Conclusions

The measurement problem has a significant influence in the correct management of the social, technical, hydraulic and economic efficiency of water companies. Since the hydraulic circuits have, normally, two flowmeters, a water balance is possible. This balances are important tools to detect leaks throughout the supply and distribution processes. If the measurement is not accurate enough, as it has occurred and described through this document, the balances do not mach. Subsequently, these tools loss their importance.

The method used to analyse the error was a procedure developed that was verified provided good results for the case studies and experiments. Nevertheless more cases need to be studied in order to assess if the procedure developed works for every case.

Regarding the CBC simulation, the most relevant conclusion regards the error calculated. The model presented an error very similar to the one verified by the tests developed

by Braga and Fernandes (2009). It may seem odd that for a error of only -1 % causes such problems. This conclusion entails a much important one, since one of the three hypotheses is happening in Asseiceira treatment plant: the facility where the outflow flowmeters are in, introduce perturbations, which leads to a large uncertainty; the outflow flowmeters may have lost accuracy; or the treatment plant loses around 4% of the raw water that arrives from Castelo do Bode dam. Through intensive interaction and discussion with the engineers responsible for the 2009 study, it was found that this fact had already been noticed without experiments and CFD analyses.

For the VFXC simulation the error calculated was of 2.53 %. This value is accordingly to the error estimated in 2009. Since in 2009, the engineers of EPAL made an intense test campaign regarding the tight of the pipe, and since it was proved that the pipe had no leaks, the conclusion reached is that the error, in this case, is due to geometry perturbations that interfere in the flow measurement.

Lastly, the errors associated to the installation and the geometry are an important and relevant issue that is not always taken into account by the engineers responsible for the design nor by the teams responsible for the installation of those equipments. If these factors are not addressed properly the flow measurement is not accurate and the several tools associated to it lose their importance.

Acknowledgement

This work could not be possible without the close collaboration between CEris (CEHIDRO) and EPAL. A special word of gratitude is due to Eng. Francisco Braga and Eng. Vitor Rocha, both of EPAL, for all the collaboration and interest.

References

Abbott, M. B., Basco, D. R., 1989. *Computational Fluid Dynamics - An Introduction of Engineers*. Longman Scientific & Technical, Harlow.

Associação Portuguesa de Distribuição e Drenagem de Águas. *Guia de Contadores Parte I - Características gerais dos contadores de água.*

Associação Portuguesa de Distribuição e Drenagem de Águas, 2000. *Guia de Contadores Parte II - Condições de Instalação e Critérios de Selecção.*

Bakewell, H. P. and Lumley, J. L., 1967. *Viscous sublayer and adjacent wall region in the turbulent pipe flow*. Phys. Fluids 10, 1880-1889.

Batchelor, G. K., 1967. *An Introduction to Fluid Dynamics*. Cambridge University Press, Cambridge, United Kingdom.

Bradshaw, P., 1973. *Effects of streamline curvature on turbulent*. AGAR - Dograph, 169, AGARD, Paris.

Braga, F. and Fernandes, M., 2009. *Analise de eventuais perdas na rede de adução da EPAL: casos de estudo.* EPAL, Lisboa.

Çengel, Y. A. and Cimbala, J. M., 2006. *Fluid Mechanics - Fundamentals and Applications*. McGraw-Hill; USA.

COMSOL 4.3, 2012. *COMSOL Multiphysics Reference Guide*. USA.

COMSOL 4.3, 2012. *COMSOL Multiphysics User's Guide*. USA.

EN 14154-2. *Water meters - Part 2: Installation and conditions of use*.

EN 14154-3. *Water meters - Part 3: Test methods and equipment.*

Fletcher C. A. J., 1991. *Computational Techniques for Fluid Dynamics*. Springer-Verlag, Berlin.

Frenzel, F., Grothey, H., Habersetzer, C., Hiatt, M., Hogrefe, W., Kirchner, M., Lütkepohl, G., Marchewka, W., Mecke, U., Ohm, M., Otto, F., Rackebrandt, K.-H., Sievert, D., Thöne, A., Wegener, H.-J., Buhl, F., Koch, C., Deppe, L., Horlebein, E., Schüssler, A., Pohl, U., Jung, B., Lawrence, H., Lohrengel, F., Rasche, G., Pagano, S., Kaiser, A. and Mutongo, T., 2011. *Industrial Flow Measurement Basics and Practice*. ABB Automation Products GmbH.

Georgescu, A.; Bernad, S., Georgescu, S.-C. and CoSoiu, I., 2007. *COMSOL Multiphysics versus FLUENT: 2D numerical simulation of the stationary flow arround a blade of the achard turbine*. 3rd Workshop on Vortex Dominated Flows, Timisoara, Romania.

Gresho, P. M., 1991. *Incompressible Fluid Dynamics: Some Fundamental Formulation Issues*. Ann. Rev. Fluid Mech., vol. 23, pp. 413-453.

Hinze, J. O., 1975. *Turbulence*. Mc-Graw-Hill, New York, USA.

ISOMAG. *Caudalímetros electromagnéticos*. Dep de Indústria e Ambiente.

Lumley, J. L., 1978. *Computational modelling of turbulent flows*. Adu. Appl. Mech., vol. 18, 123-176.

Lumley, J. L., 1992. *Some comments on turbulence*. Phys. Fluids A 4, 203-211.

MET-FLOW, 2014. *UVP - DUO Monitor User's Guide*. Switzerland.

Novais-Barbosa, J., 1985. *Mecânica dos fluidos e hidráulica geral*. Porto Editora.

Pope, S. B., 2000. *Turbulent Flows*. Cambridge University Press; Cambridge, United Kingdom.

Quintela, A. C., 2002. *Hidráulica*. Fundação Calouste Gulbenkian, Lisboa.

Speziale, C. G., 1987. *On nonlinear k-l and k-ε models of turbulence*. J. Fluid Mech. 178, 459-475.

Tenneks, H. and Lumley, J. L., 1972. *A First Course in Turbulence*. MIT Press, Cambridge MA, USA.

Tritton, D. J., 1988. *Physical Fluid Dynamics*. Oxford University Press, United Kingdom.

Versteeg, H. K. and Malalasekera, W., 2007. *An Introduction to Computational Fluid Dynamics: the finite volume method*. Pearson Education Limited, England.

White, F. M., 1991. *Viscous fluid flow*. McGraw-Hill, USA.

Wosnik, M., Castillo, L. and George, W. K., 2000. *A theory for turbulent pipe and channel flows*. J. Fluid Mech., vol. 421, pp. 115-145.